HHS Public Access

Author manuscript

Science. Author manuscript; available in PMC 2018 May 22.

Published in final edited form as:

Science. 2017 April 14; 356(6334): 197–200. doi:10.1126/science.aam6512.

Nanoscale-length control of the flagellar driveshaft requires hitting the tethered outer membrane

Eli J. Cohen[1], **Josie L. Ferreira**[2], **Mark S. Ladinsky**[3], **Morgan Beeby**[2], and **Kelly T. Hughes**[1,*]

[1]Department of Biology, University of Utah, Salt Lake City, UT 84112, USA

[2]Department of Life Sciences, Imperial College of London, London SW7 2AZ, UK

[3]Division of Biology and Biological Engineering 114-96, California Institute of Technology, Pasadena, CA 91125, USA

Abstract

The bacterial flagellum exemplifies a system where even small deviations from the highly regulated flagellar assembly process can abolish motility and cause negative physiological outcomes. Consequently, bacteria have evolved elegant and robust regulatory mechanisms to ensure that flagellar morphogenesis follows a defined path, with each component self-assembling to predetermined dimensions. The flagellar rod acts as a driveshaft to transmit torque from the cytoplasmic rotor to the external filament. The rod self-assembles to a defined length of ~25 nanometers. Here, we provide evidence that rod length is limited by the width of the periplasmic space between the inner and outer membranes. The length of Braun's lipoprotein determines periplasmic width by tethering the outer membrane to the peptidoglycan layer.

Length determination of linear filaments poses a particular problem, some of whose known examples are solved by using molecular rulers. The bacterial flagellum is one such linear filament composed of a series of axial structures that must be assembled to precise specifications to enable motility. The bacterial flagellum consists of a cytoplasmic, ion-powered rotary motor connected to a driveshaft (rod) that transmits torque to the external filament (propeller). The rod extends ~25 nm from the inner membrane through the peptidoglycan layer and periplasmic space to the outer membrane and terminates (Fig. 1). Termination of rod assembly positions the rod tip perpendicular to the outer membrane permitting an outer membrane–bound bushing complex, the periplasmic lipopolysaccharide ring (PL-ring), to assemble around the rod. The PL-ring forms an outer-membrane pore and results in the initiation of hook polymerization, which extends ~55 nm, followed by the filament. The hook acts as a universal joint connecting the rigid rod to the rigid filament, whose rotation propels the bacterium forward and allows the cell to alter its swimming trajectory (Fig. 1) (1–5). The length-control mechanism of the hook is well characterized and depends on the action of a secreted, molecular ruler, FliK. When the hook reaches a minimal length, the C terminus of FliK that is in the process of being secreted through the

*Corresponding author. hughes@biology.utah.edu.

SUPPLEMENTARY MATERIALS

www.sciencemag.org/content/356/6334/197/suppl/DC1 Materials and Methods

growing flagellar structure interacts with the FlhB gatekeeper protein of the flagellar type III secretion apparatus to switch secretion-substrate specificity from early, rod-hook secretion mode to late, filament secretion mode (6–10).

Although the flagellar hook serves as an excellent model for understanding length determination via the FliK molecular ruler, the length-control mechanism of another flagellar component, the rod, has remained enigmatic (11). The rod consists of two distinct substructures: the ~7-nm proximal and ~18-nm distal rod (12–14). The proximal rod is composed of four different proteins, and its mechanism of assembly remains unknown. In contrast, the distal rod is composed of ~50 copies of a single protein, FlgG. FlgG subunits must stack upon one another to reach the outer membrane (14). The self-stacking capability of FlgG poses a dilemma for the cell: Once initiated, what prevents continuously secreted FlgG subunits from polymerizing indefinitely?

A model for flagellar rod-length control was proposed on the basis of a set of mutations mapping to the *flgG* gene (*flgG** mutations) that resulted in increased rod lengths. The *flgG** rods grow beyond the wild-type (WT) length of ~25 nm to ~60 nm, which is determined by the FliK ruler (15). Because the *flgG** mutations resulted in extended distal rod growth, a rod length–control mechanism was proposed that depended on intrinsic FlgG subunit stacking interactions during distal rod assembly. This model was based on earlier reports that the distal rod consisted of ~26 FlgG subunits, which would constitute two stacks of FlgG in the distal rod (16). Recent work has determined that the number of FlgG subunits in the distal rod is actually ~50 (14), which does not support an intrinsic distal rod length–control model based on subunit stacking interactions.

The FlgG-intrinsic model for rod-length control predicted that rod length would be unaffected by the cytoplasmic FlgG concentration. However, overexpression of the *flgG* gene yielded an increase in the average rod length (Fig. 2). This result and the finding that the distal rod is composed of ~50 FlgG subunits forced us to explore other possible mechanisms of flagellar rod-length control.

A clue to the actual rod-length control mechanism came from the isolation of suppressor mutations of the *flgG** length-control mutants. Because rod growth in these mutants continues to ~60 nm, we speculated that the placement of the rod tip was no longer perpendicular to the outer membrane, compromising PL-ring assembly and resulting in filament growth in the periplasm and a nonmotile phenotype (11, 17). The nonmotile phenotype of *flgG** mutants allowed us to perform a selection for suppressor mutations that relieved these mutants of the motility defect. One class of mutants arose in a gene not previously implicated in flagellar morphogenesis, *lppA*.

The *lppA* gene encodes Braun's lipoprotein, which is the major outer-membrane lipoprotein of the cell in Gram-negative bacteria. Lpp is the most abundant protein in *Escherichia coli*, with 10^6 copies per cell. The LppA protein is secreted to the periplasm and processed to a final length of 58 amino acids that form homotrimers. N-terminal cysteine residues are acylated and anchor the LppA trimer in the outer membrane, whereas C-terminal lysine residues are covalently attached to the peptidoglycan layer (fig. S1) (18–20). Unlike the case

in WT *Salmonella*, which displays a slight reduction in motility upon deletion of *lppA* (fig. S2), the *flgG** mutants exhibited a 2- to 3-fold increase in swim diameter on motility agar when *lppA* was deleted (fig. S3).

We hypothesized that without LppA, the space between the peptidoglycan and outer membrane would be less constricted and would allow *flgG** distal rods to be positioned perpendicular to the outer membrane as they grew longer than 25 nm, which would permit PL-ring pore formation. This predicted that the number of extracellular filaments assembled by *flgG** mutants would increase upon deletion of *lppA*. Western blot analysis and fluorescence microscopy confirmed that extracellular flagellin secretion and assembly in *flgG** mutants increased in the absence of LppA (fig. S4). Additionally, *flgG** mutants still produced abnormally long rods regardless of whether LppA was present or not (fig. S5). These data suggested that the outer membrane acts as a barrier to distal rod growth and prevents continuous rod polymerization.

Unlike *E. coli*, *Salmonella* has two tandem *lpp* genes, *lppA* and *lppB* (fig. S1) (21, 22). The LppA protein is the equivalent of *E. coli* Lpp, whereas *lppB* is not expressed under standard laboratory conditions (23). LppA-length variants were constructed to test whether LppA determined the spacing between the peptidoglycan and outer membrane and whether this spacing determined distal rod length. LppA trimer formation is driven by hydrophobic interactions between seven heptad-repeat motifs within the mature 58–amino acid LppA monomers (20). An initial attempt to increase Lpp length by fusing LppA and LppB resulted in cells severely defective in cell shape and division (fig. S1). The LppA structure is based on heptad repeats of interacting monomers in the trimer. In an attempt to prevent cell-shape and division defects, length variants were designed that maintained interacting heptad repeats. The LppA length variants constructed included a 21–amino acid deletion and three longer variants containing insertions of 21, 42, and 63 residues (fig. S6).

To determine whether changing LppA length resulted in a concomitant change in peptidoglycan-to–outer-membrane distance, LppA length–variant cells were embedded in resin and analyzed by electron microscopy. We observed changes in peptidoglycan-to–outer-membrane spacing that were proportional to LppA lengths (Fig. 3, A and B). Electron cryomicroscopy (cryo-EM), which preserved cells in a near-native frozen-hydrated state, corroborated these results. Imaging cells harboring $lppA^{-21}$, $lppA^{+21}$, and $lppA^{WT}$ variants by using cryo-EM demonstrated that the length of LppA was a principal determinant of the inner-membrane–to–outer-membrane distance (Fig. 3C and fig. S7).

To test whether the length of the flagellar rod was dictated by periplasmic width, we measured rods isolated from the LppA-length mutants. We observed changes in the average length of the flagellar rod as the length of LppA changed (Fig. 3, D and E, and figs. S8 and S9). Taken together, the data obtained from resin-embedded electron microscopy, cryo-EM, and rod-length measurements were consistent with a model for distal rod–length control that required contact with the outer membrane.

Electron cryo-EM was then used to address whether the osmotic pressure in the periplasm mirrors that of the cytoplasm or the external environment. Suppression of the *flgG** motility

defect by loss of LppA is consistent with the osmolalities in the cytoplasm and periplasm being equal, which is in agreement with previous studies (24, 25). In an attempt to further address this, we imaged one mutant having *lppAB* deleted and one with both *lppAB* and *pal* deleted. Pal is another abundant outer-membrane lipoprotein that noncovalently binds peptidoglycan (26, 27) and could tether the outer membrane to the peptidoglycan. We reasoned that if LppA functions as a tether under tension, as expected if the cytoplasmic and periplasmic osmolalities were equal, the absence of LppA would allow the outer membrane to pull away from the cell body as the osmolality of the periplasm equilibrates with that of the external environment.

Imaging the Δ*lppAB* mutant revealed that the outer membrane pulled away from the cell body in taut blebs. In the Δ*lppAB* Δ*pal* double mutant, more extreme blebbing was observed (Fig. 4 and fig. S7). These results support previous reports that the osmolality of the periplasm mirrors that of the cytoplasm and that the function of LppA (and perhaps other peptidoglycan-binding lipoproteins) is to act as a tether rather than a support column under normal growth conditions.

Evolution places constraints and limitations on each component of an organism in order to maximize the fitness of the organism as a whole. In addition to housing the flagellar driveshaft, the periplasm contains a multitude of other cellular machinery. We were surprised to discover that addition of 21 residues to LppA increased the apparent swim rate of *Salmonella* to a small degree (~10%) (fig. S10). Also, altering the length of LppA caused slower growth and morphological abnormalities that became more pronounced the further the length deviated from the mature wild-type LppA length of 58 residues (fig. S10). These observations suggest that the selective forces that have influenced flagellar form and function have led to a compromise on the absolute optimization of swimming ability in favor of a motility organelle that is optimized to function in harmony with other components of the cell and under various conditions.

Supplementary Material

Refer to Web version on PubMed Central for supplementary material.

Acknowledgments

We thank T. Silhavy for anti-Lpp antisera and D. Blair and N. Wingreen for helpful discussions. All strains, primers, and plasmids used in this study are available upon request. This work was funded by NIH grant GM056141 (K.T.H.), Marie Curie Career Integration Grant 630988 (M.B.) and UK Medical Research Council Ph.D. Doctoral Training Partnership award MR/K501281/1 (J.L.F.).

REFERENCES AND NOTES

1. Macnab RM. Annu Rev Microbiol. 2003; 57:77–100. [PubMed: 12730325]
2. Chevance FFV, Hughes KT. Nat Rev Microbiol. 2008; 6:455–465. [PubMed: 18483484]
3. Jones CJ, Homma M, Macnab RM. J Bacteriol. 1989; 171:3890–3900. [PubMed: 2544561]
4. Schoenhals GJ, Macnab RM. J Bacteriol. 1996; 178:4200–4207. [PubMed: 8763949]
5. Berg HC, Anderson RA. Nature. 1973; 245:380–382. [PubMed: 4593496]
6. Hirano T, Yamaguchi S, Oosawa K, Aizawa S. J Bacteriol. 1994; 176:5439–5449. [PubMed: 8071222]

7. Erhardt M, Singer HM, Wee DH, Keener JP, Hughes KT. EMBO J. 2011; 30:2948–2961. [PubMed: 21654632]
8. Muramoto K, Makishima S, Aizawa SI, Macnab RM. J Mol Biol. 1998; 277:871–882. [PubMed: 9545378]
9. Uchida K, Aizawa S. J Bacteriol. 2014; 196:1753–1758. [PubMed: 24563036]
10. Takahashi N, et al. J Bacteriol. 2009; 191:6469–6472. [PubMed: 19666714]
11. Chevance FFV, et al. Genes Dev. 2007; 21:2326–2335. [PubMed: 17761814]
12. Homma M, Kutsukake K, Hasebe M, Iino T, Macnab RM. J Mol Biol. 1990; 211:465–477. [PubMed: 2129540]
13. Saijo-Hamano Y, Uchida N, Namba K, Oosawa K. J Mol Biol. 2004; 339:423–435. [PubMed: 15136044]
14. Fujii T, et al. Nat Commun. 2017; 8:14276. [PubMed: 28120828]
15. Hirano T, Mizuno S, Aizawa S, Hughes KT. J Bacteriol. 2009; 191:3938–3949. [PubMed: 19376867]
16. Jones CJ, Macnab RM, Okino H, Aizawa S. J Mol Biol. 1990; 212:377–387. [PubMed: 2181149]
17. Cohen EJ, Hughes KT. J Bacteriol. 2014; 196:2387–2395. [PubMed: 24748615]
18. Braun V. Biochim Biophys Acta. 1975; 415:335–377. [PubMed: 52377]
19. Kovacs-Simon A, Titball RW, Michell SL. Infect Immun. 2011; 79:548–561. [PubMed: 20974828]
20. Shu W, Liu J, Ji H, Lu M. J Mol Biol. 2000; 299:1101–1112. [PubMed: 10843861]
21. Sha J, et al. Infect Immun. 2004; 72:3987–4003. [PubMed: 15213144]
22. Fadl AA, et al. Infect Immun. 2005; 73:1081–1096. [PubMed: 15664952]
23. Kröger C, et al. Cell Host Microbe. 2013; 14:683–695. [PubMed: 24331466]
24. Cayley DS, Guttman HJ, Record MT Jr. Biophys J. 2000; 78:1748–1764. [PubMed: 10733957]
25. Sochacki KA, Shkel IA, Record MT, Weisshaar JC. Biophys J. 2011; 100:22–31. [PubMed: 21190653]
26. Cascales E, Bernadac A, Gavioli M, Lazzaroni JC, Lloubes R. J Bacteriol. 2002; 184:754–759. [PubMed: 11790745]
27. Parsons LM, Lin F, Orban J. Biochemistry. 2006; 45:2122–2128. [PubMed: 16475801]
28. Nambu T, Minamino T, Macnab RM, Kutsukake K. J Bacteriol. 1999; 181:1555–1561. [PubMed: 10049388]

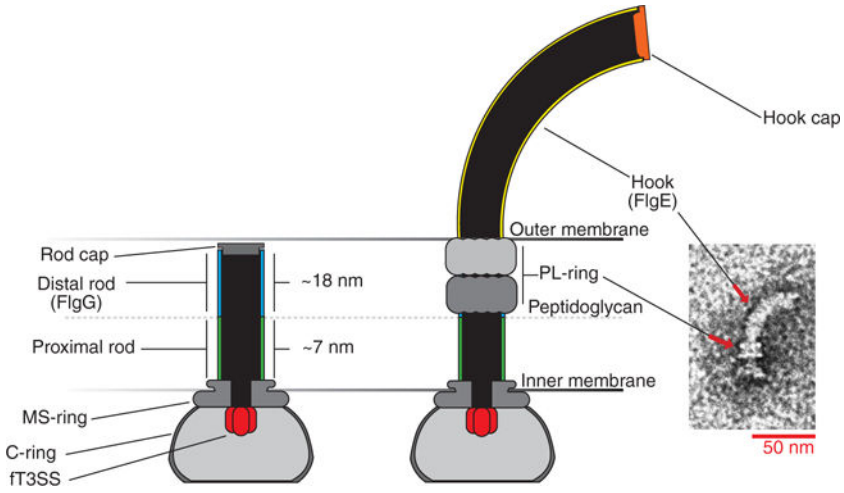

Fig. 1. The hook basal body of *Salmonella enterica*

Construction of the flagellum begins with the assembly of the transmembrane membrane supramembrane ring (MS-ring), the flagellar type 3 secretion system (fT3SS), and the cytoplasmic ring (C-ring) rotor complex. The proximal rod polymerizes on top of the MS-ring followed by the FlgG distal rod to span the distance between the peptidoglycan layer and the outer membrane. FlgJ, the rod cap, allows the growing structure to pass through the peptidoglycan layer through localized hydrolysis of the peptidoglycan (28). Once the distal rod has reached the outer membrane, formation of the periplasmic ring–lipopolysaccharide ring (P-ring–L-ring) complex simultaneously forms a hole in the outer membrane and dislodges the rod cap. Rod cap removal allows the hook cap (FlgD) to form on the tip of the nascent structure and to promote assembly of the hook by FlgE subunits.

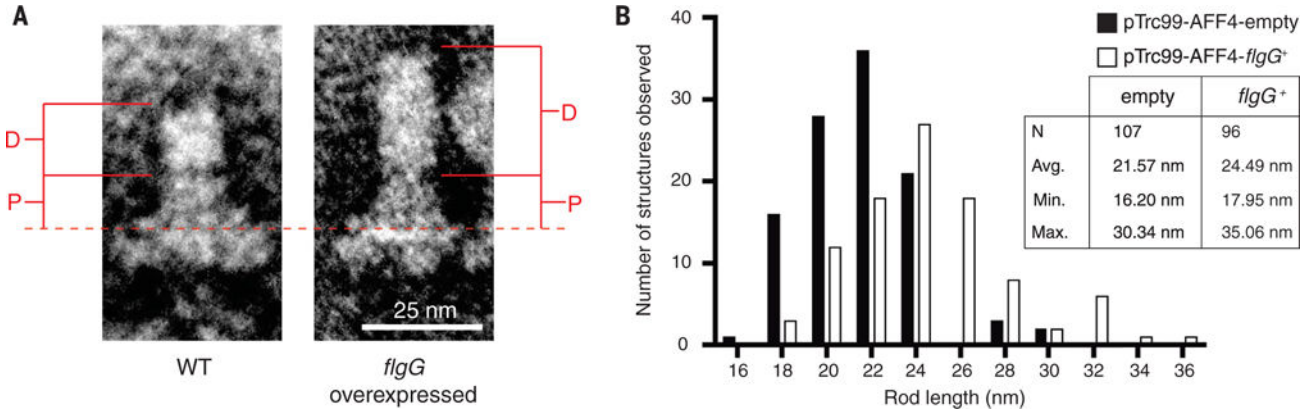

Fig. 2. Overexpression of *flgG* resulted in longer distal rods

To test the FlgG intrinsic model for length control of the distal rod, *flgG* was overexpressed from a plasmid vector to supplement *flgG* expression from its native chromosomal locus in a strain lacking the genes required for termination of distal rod assembly (*flgH*) and subsequent hook assembly (*flgD* and *flgE*). (**A**) Flagellar basal bodies were purified from the *flgG*-overexpression background and compared with those from an empty-vector control strain by transmission electron microscopy (TEM). (**B**) Measurements were taken from the top of the MS-ring [dashed line in (A)] to the tip of the rod (P, proximal rod; D, distal rod). Overexpression of *flgG* was found to significantly increase the length of the rod ($P < 0.0001$, Student's two-tailed t test, $N = 2$).

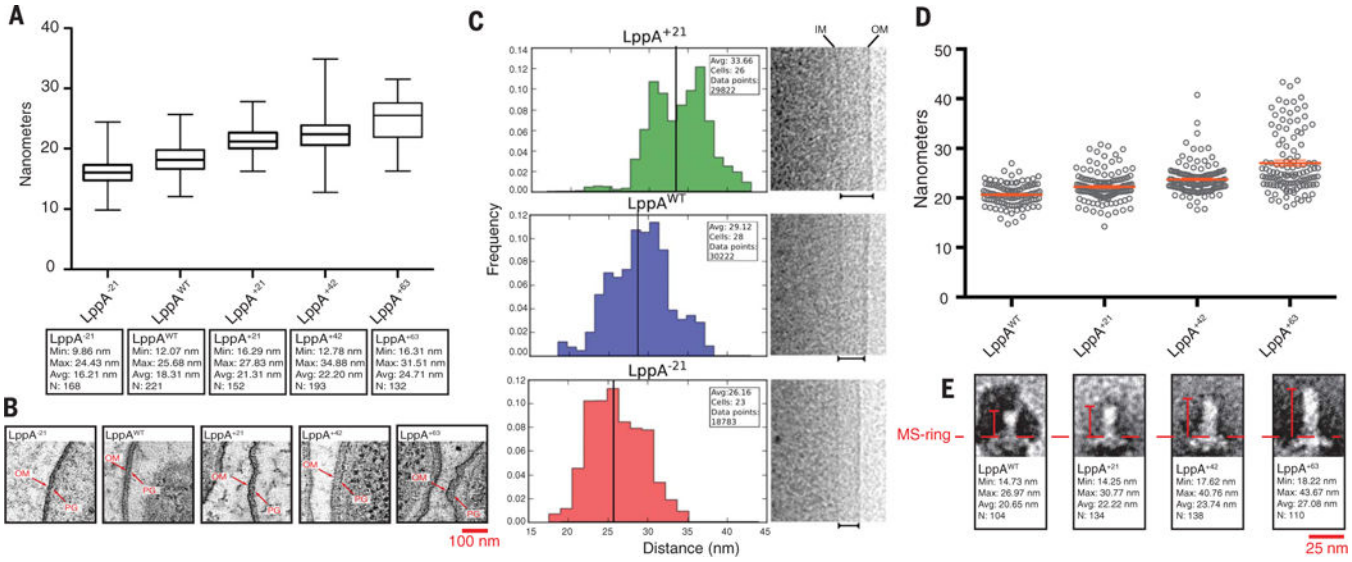

Fig. 3. The inner-to outer-membrane distance and flagellar rod length varied with LppA lengths

Resin-embedded LppA-length mutants, as well as WT control (TH22579 and TH22634 to TH22637) were thin-sectioned and observed by electron tomography. (**A** and **B**) The peptidoglycan-layer (PG)–to–outer-membrane (OM) distances for each strain were measured. As the length of LppA increased, we observed a corresponding increase in PG-to-OM distance [$P < 0.0001$, one-way analysis of variance (ANOVA)]. (**C**) To verify these results, cells from −21, +21, and WT LppA strains (TH22579, TH22634, and TH22635) were imaged via cryo-EM, and the distances between the inner membrane (IM) and OM were measured for each. The distances varied with LppA lengths ($P < 0.0001$, Student's two-tailed *t* test). (**D** and **E**) Flagellar rods from lengthened LppA variants (TH22574 to TH22577) were purified, imaged via TEM and measured. The average length of the rod increased ~1.5 to 2 nm for every three heptad repeats (21 residues) added [$P < 0.0001$, one-way ANOVA, $N = \geq 3$, data in (D) are means ± SEM].

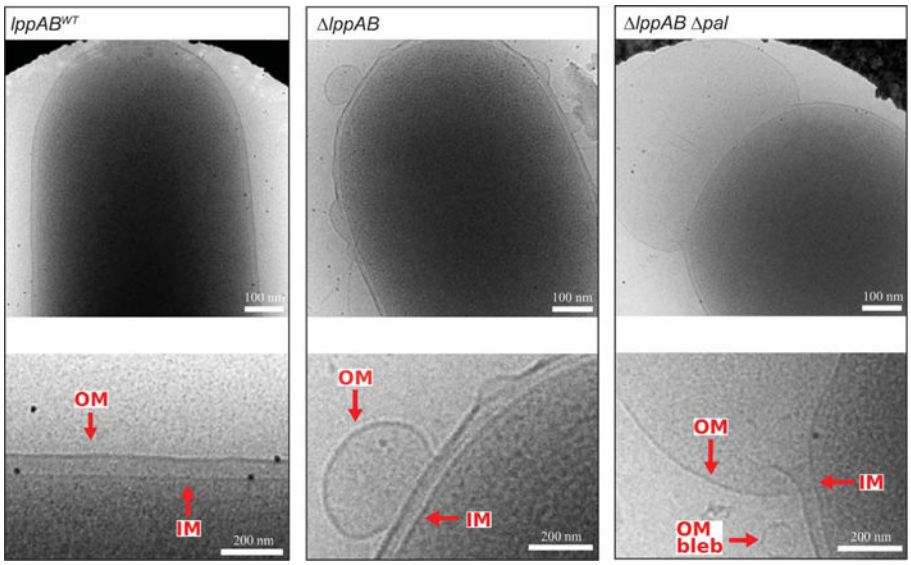

Fig. 4. LppA functions as an outer-membrane tether

Deletion of *lppAB* (strain TH22543) resulted in the formation of taut outer-membrane blebs that pulled away from the cell body. The severity of blebbing was increased in the Δ*lppAB* Δ*pal* double mutant (strain TH22569).